Theoretical and Applied Climatology (2019) 137:2109–2123
https://doi.org/10.1007/s00704-018-2728-6

ORIGINAL PAPER

Kinematic and thermodynamic conditions related to convective systems with a bow echo in Poland

Daniel Celiński-Mysław[1] · Angelika Palarz[1] · Łukasz Łoboda[2]

Received: 22 August 2018 / Accepted: 25 November 2018 / Published online: 5 December 2018

Abstract
Severe wind events are often related to the occurrence of mesoscale convective systems with arch-shaped radar reflectivity, i.e., a bow echo. In this research, the kinematic and thermodynamic conditions associated with 91 bow echo cases which occurred in the warm season (i.e., from early April until late September) in Poland (2007–2014) were analyzed. The environmental conditions were determined primarily based on the upper air soundings, and additionally on data obtained from ERA-Interim reanalysis. The results indicate that there is a relatively wide range of shear and instability environments associated with bow echoes over Poland. The identified cases occurred both in weakly forced environments, and as well developed in dynamic synoptic patterns with low instability. We have also found cases with strong instability and significantly increased shear values. The combination of a moist boundary layer and steep mid-tropospheric lapse rate usually resulted in moderate to high CAPE values for identified bow echo cases. The median of surface-based CAPE was equal to 1594 J/kg (Mean Layer CAPE = 1038 J/kg) for soundings, and to 1622 J/kg (Mean Layer CAPE = 1275 J/kg) for ERA-Interim. Bow echo environments also showed significantly increased potential for strong downdrafts and damaging outflow winds (the median Downdraft CAPE reached 849 J/kg for soundings and 734 J/kg for ERA-Interim). Bow echoes were usually associated with the occurrence of strong air flow in the troposphere. The presence of a jet stream in the middle and upper troposphere contributed to the development of increased vertical wind shear values. The median of 0–6-km shear exceeded 15 m/s, whereas for 0–3-km shear, it was approximately equal to 12.5 m/s and to 7 m/s for 0–1-km shear.

1 Introduction

Mesoscale convective systems (MCSs) can pose a significant risk to human life and health, as well as huge losses in the economy. Every year across Europe, several thousand destructive wind, tornado, hail, or heavy rain events cause temporary disorganization of life. These phenomena are frequently connected with the movement of strong meso-β-scale convective systems with arch-shaped radar reflectivity, i.e., bow echo. According to Klimowski et al. (2003), at least 29% of all severe wind reports recorded in the USA (Northern High Plains) during the warm seasons of 1996–1999 were caused by the activity of convective systems with a bow echo (24% of fatal/deadly nontornadic convective wind storms in the USA from 1998 to 2007 (all seasons)—Schoen and Ashley 2011). Gatzen (2013), in turn, pointed out that 58% of severe wind reports (≥ 26 m/s) in Germany were related to a bow echo (for the warm season between 1997 and 2011).

Research on the spatial and temporal variability of bow echo occurrence focused primarily on the area of the USA and Central Europe. They included both warm season (Klimowski et al. 2004; Adams-Selin and Johnson 2010; Celiński-Mysław and Palarz 2017), and cool season bow echo cases (Burke and Schultz 2004; Klimowski et al. 2004; Adams-Selin and Johnson 2010). However, publications in which the causes of bow echo development were analyzed dominate in the world literature (e.g., Argentina, Torres Brizuela et al. 2011; Belgium and Germany, Mathias et al. 2017; China, Peng et al. 2013; Finland, Punkka et al. 2006; France, Ribaud et al. 2016; India, Devajyoti et al. 2014; Spain, Lopez 2007; USA, Xu et al. 2015).

✉ Daniel Celiński-Mysław
daniel.celinski-mysław@doctoral.uj.edu.pl

Angelika Palarz
angelika.palarz@doctoral.uj.edu.pl

Łukasz Łoboda
lukaszloboda89@gmail.com

[1] Department of Climatology, Jagiellonian University, Gronostajowa 7, 30-387 Krakow, Poland

[2] Solarwinds Poland Sp. z o.o., Puszkarska 7J, 30-644 Krakow, Poland

The development modes, dynamics, structure, types, and conditions associated with bow echoes were determined based both on observations (Klimowski et al. 2004; Gatzen 2013; Celiński-Mysław and Matuszko 2014; Celiński-Mysław and Palarz 2017), and on numerical simulations (Weisman 1993; James et al. 2006; Atkins and St Laurent 2009; French and Parker 2014). Previous research showed evidence that irrespective of the area of occurrence, convective systems with a bow echo develop primarily as a result of squall line transformation or the combining of often weakly organized convective cells. The predominant bow echo types included classic bow echo and bow-echo complex (Klimowski et al. 2003, 2004; Celiński-Mysław and Palarz 2017).

Studies on bow echoes focus particularly on two aspects: (1) on the kinematic, thermodynamic, and synoptic conditions accompanying their development (Burke and Schultz 2004; Adams-Selin and Johnson 2010); and (2) the mechanisms that are accountable for the occurring of severe wind gusts (Fujita 1978; Weisman 1992, 1993; Przybylinski 1995; Wakimoto et al. 2006a; Atkins and St Laurent 2009; Xu et al. 2015). Most of the studies that examined the conditions favorable for bow echo formation concentrated on the sensitivity of bow echo cases to kinematic, particularly the low-level (LLS) and mid-level shear (MLS) (e.g., Weisman 1993; Burke and Schultz 2004; Coniglio et al. 2004; Chen et al. 2007; Atkins and St Laurent 2009), and thermodynamic parameters, especially the magnitude of convective available potential energy (CAPE) (e.g., Weisman 1993; Evans and Doswell III 2001; Klimowski et al. 2003). Their values strongly depend on the season. Cool season bow echoes are driven mainly by strong vertical wind shears accompanied by low to moderate instability (Evans and Doswell III 2001; Burke and Schultz 2004). By contrast, in the warm season, thermodynamic conditions play a decisive role in the development of deep convection and bow echoes (Johns and Hirt 1987; Klimowski et al. 2003; Celiński-Mysław and Matuszko 2014). James et al. (2006), utilizing a storm-scale numerical model, made an assessment of bow echo sensitivity to environmental moisture. The authors demonstrated strong bow echo sensitivity to the ambient water vapor mixing ratio which is similar to that of Burke and Schultz (2004). James et al. (2006) showed relatively dry conditions in the lower and middle troposphere conducive to the formation of colder downdrafts and strong cold pool development leading to upshear-tilted convection and initiating processes that cause the growth and intensification of the bowing segment. Furthermore, for instance, Celiński-Mysław and Matuszko (2014), and Zhao et al. (2015), pointed out the importance of a mid-tropospheric trough on the development of powerful convective systems with a bow echo and derecho (a large-scale and persistent zone of strong straight-line wind caused typically by a MCS with a bow echo, where high wind speeds are an effect of strong downdrafts reaching the surface—downbursts). They showed that the divergence zone of a trough can contribute to the deepening of a depression and to the intensification of processes active along the squall line.

There are two hypotheses that explain the causes of strong and destructive straight-line (nontornadic) winds occurring within bow echoes. One of them states that the descending rear-inflow jet (RIJ) and strong downdrafts reaching the surface are primarily responsible for the damaging winds (Fujita 1978; Rotunno et al. 1988; Weisman 1992; Peng et al. 2013). The other one in turn suggests that severe winds are connected with low-level meso-γ-scale vortices located within a bow echo (Weisman and Trapp 2003; Trapp and Weisman 2003; Wakimoto et al. 2006a; Wheatley et al. 2006). Both hypotheses were confirmed in studies conducted by, among others, Wakimoto et al. (2006b), Atkins and St Laurent (2009), Xu et al. (2015), and Mathias et al. (2017). They proved that the strongest wind damage is associated with mesovortices, which are embedded in the system RIJ. Atkins and St Laurent (2009), analyzing damaging potential and genesis of low-level meso-γ-scale vortices within bow echoes, found also that mesovortices are strongest for moderate-to-strong LLS. Similar results were presented in the studies conducted by, among others, Weisman and Trapp (2003), Trapp and Weisman (2003), and Xu et al. (2015).

This study provides a description of the environmental conditions associated with bow echo cases (favorable to their development) that occurred over Poland in the warm season between 2007 and 2014. The main objective of the paper is to identify the values of kinematic and thermodynamic parameters that are conducive to bow echo development in Poland. The remainder of the paper is organized as follows: Sect. 2 gives a description of the data (upper air soundings and ERA-Interim reanalysis) and methods, Sect. 3 shows the results and Sect. 4 the discussion. The conclusion are presented in Sect. 5.

2 Data and methods

The determination of environmental conditions accompanying the bow echo was conducted with respect to the identified warm season cases that developed in the years 2007–2014 over Poland (Fig. 1). We adopted the same identification criteria as in Celiński-Mysław and Palarz (2017). These conditions were defined by the values of kinematic and thermodynamic parameters (Table 1). Environmental features were identified primarily based on sounding-derived data (e.g., as in Kolendowicz et al. 2017; Taszarek et al. 2018), and additionally based on data obtained from ERA-Interim reanalysis (e.g., as in Kaltenboeck and Steinheimer 2015; Westermayer et al. 2016a). Temperature and moisture conditions near the surface were determined based on synoptic station observations as well.

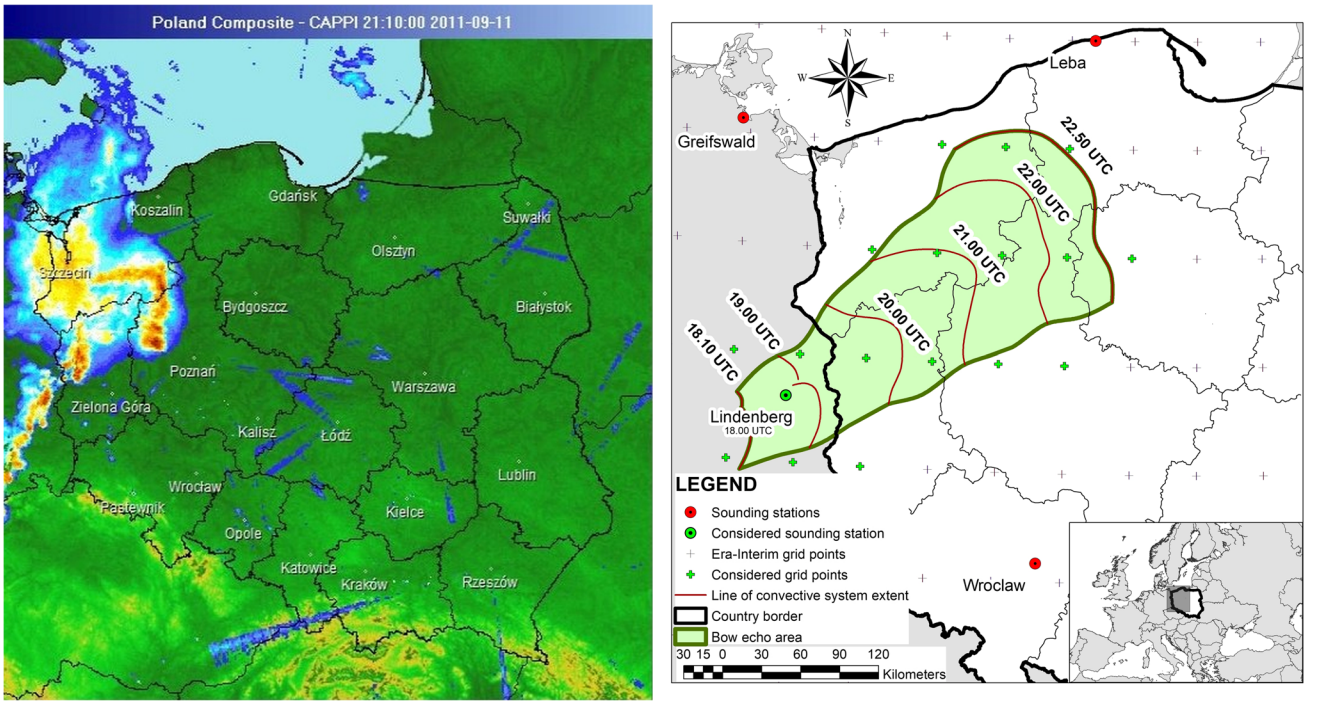

Fig. 1 A bow echo event on 11 September 2011. On the left, the radar depiction of a convective system with a bow echo—CAPPI product (From Centre for Ground Based Remote Sensing, Institute of Meteorology and Water Management – National Research Institute). On the right, the schema of the system movement along with selected sounding and grid points that were considered/analyzed for this bow echo case

Upper air soundings from 11 radiosonde stations were utilized. The data were available at 00 and 12 UTC for Budapest, Greifswald, Kaliningrad, Leba, Legionowo, Lviv, Poprad, Prostejov, and Wroclaw, whereas for Lindenberg, Prague, and Vienna additionally at 06 and 18 UTC (Fig. 2). In order to select an appropriate station from which the data was used, we assumed the following criteria:

– The sounding sampled the same air masses that gave rise to and sustained the bow echo thunderstorm (e.g., in Brooks et al. 1994—tornado thunderstorm).
– The sounding was close in time and space to the identified bow echo area (Fig. 1).

- Maximum 200 km from this area (e.g., Taszarek and Kolendowicz 2013—from tornado)—more than 200 km (up to 250 km), when a bow echo occurred around 06 and 18 UTC, and soundings from Prague, Lindenberg, and Vienna could be used (these soundings represented well the time of the bow echo occurrence).
- A bow echo event takes place up to 2 h prior to and 6 h after the sounding time (in Taszarek et al. 2017 up to 2 h prior to and 4 h after).

– The sounding with MLCAPE exceeded 50 J/kg (e.g., Klimowski et al. 2003).
– The sounding should not be contaminated by convection (e.g., Burke and Schultz 2004; Cohen et al. 2007).

Applying these criteria, the upper air analyses were limited to 79 out of a possible 91 bow echo cases. For the cases when more than one sounding met the assumptions (13 cases), the upper air data from all of the stations located close to the potential bow echo area were analyzed. This particularly concerned the cases with the largest size. Consequently, we examined the parameter values for 93 soundings. For only one case, the assumed criteria have been met by three soundings. For each of the remaining 12 cases, we have analyzed two soundings. A lower threshold of the maximum distance from the bow echo area significantly reduces the sample size of the upper air soundings. Considering the threshold of 80 km (e.g., Kerr and Darkow 1996; Potvin et al. 2010), 60 soundings for 52 bow echoes might be analyzed. However, the differences between the median values of the selected parameters obtained from the threshold 80 and 200 km are not significant (not shown).

Additionally, given the limitations of sounding-derived data, e.g., soundings were too far out in space and time from thunderstorm events, data obtained from ERA-Interim reanalysis were also applied (Dee et al. 2011). The temporal resolution of the data is 6 h—00, 06, 12, and 18 UTC—whereas the spatial resolution is 0.75° × 0.75° (Fig. 2). In order to compute the parameter values, information from the pressure levels and the hybrid-sigma levels of the L60 model were used. The values of kinematic and thermodynamic parameters were calculated for each grid point situated within the bow echo area (and close to this area—neighboring grid points) (Fig. 1). The

Table 1 Parameters used in the study, including their units, abbreviations, and references

Parameter	Units	Abbreviation	Used among others in
Moisture parameter			
Mean mixing ratio in the lowest 50 hPa	g/kg	MIXR	Klimowski et al. 2003 (in the lowest 1000 m); Púčik et al. 2011; Taszarek et al. 2017 (in the lowest 500 m)
Temperature parameters			
Surface temperature (2 m temperature)	°C	ST	Adams-Selin and Johnson 2010; Hamid 2012; Celiński-Mysław and Matuszko 2014
800–500 hPa temperature lapse rate	°C/km	tLR800-500	Brooks et al. 2003 (700–500 hPa); Burke and Schultz 2004 (850–500 hPa); Taszarek et al. 2017
Parcel parameters			
Surface-based convective available potential energy	J/kg	SBCAPE	Klimowski et al. 2003; Taszarek and Kolendowicz 2013; Celiński-Mysław and Matuszko 2014
Surface-based convective inhibition	J/kg	SBCIN	Klimowski et al. 2003; Romero et al. 2007
Surface-based lifting condensation level	m	SBLCL	Klimowski et al. 2003
50 hPa mean layer convective available potential energy	J/kg	MLCAPE	Mathias et al. 2017; Taszarek et al. 2018 (0–500 m AGL mixed layer)
50 hPa mean layer convective inhibition	J/kg	MLCIN	Mathias et al. 2017
50 hPa mean layer lifting condensation level	m	MLLCL	Taszarek et al. 2017 (0–500 m AGL mixed layer)
Most unstable convective available potential energy	J/kg	MUCAPE	Evans and Doswell III 2001; Burke and Schultz 2004; Mathias et al. 2017
Most unstable convective inhibition	J/kg	MUCIN	Mathias et al. 2017
Most unstable lifting condensation level	m	MULCL	Burke and Schultz 2004; Púčik et al. 2015
Downdraft convective available potential energy	J/kg	DCAPE	Evans and Doswell III 2001; Celiński-Mysław and Matuszko 2014; Púčik et al. 2015
Kinematic parameters			
0–1 km vertical wind shear (low-level shear)	m/s	LLS	Gatzen et al. 2011; Taszarek and Kolendowicz 2013; Púčik et al. 2015
0–3 km vertical wind shear (mid-level shear)	m/s	MLS	Evans and Doswell III 2001; Klimowski et al. 2003; Burke and Schultz 2004 (0–2.5 km); Taszarek et al. 2017
0–6 km vertical wind shear (deep-layer shear)	m/s	DLS	Evans and Doswell III 2001; Burke and Schultz 2004; Mathias et al. 2017; Taszarek et al. 2017
The presence of the upper jet (wind speed ≥ 30 m/s in the 400–200-hPa layer)	–	Upper jet	Taszarek and Kolendowicz 2013 (≥ 35 m/s in the 400–200 hPa layer)
The presence of the lower jet (wind speed ≥ 20 m/s in the 800–500-hPa layer)	–	Lower jet	Taszarek and Kolendowicz 2013 (≥ 25 m/s in the 800–500-hPa layer)

closest reanalysis output time was always selected for describing the conditions of bow echo occurrence (up to 6 h before a bow echo). The Sounding and Hodograph Analysis and Research Program in Python (SHARPpy—Blumberg et al. 2017) and R software (R Development Core Team 2008) were used for calculating the values of the parameters (both in the case of sounding and of reanalysis data). Previously, the SHARPpy software package was used also by, e.g., King and Kennedy (2018) who investigated how reanalyses (Era-Interim, NARR, MERRA-2, JRA-55) represent North American supercell environments, and by Miller and Mote (2018), who examined conditions associated with weakly forced and pulse thunderstorm in the Southeast USA.

As indicated by Weisman and Klemp (1982), Johns and Doswell III (1992), and many others, the crucial ingredients for deep convection development, likewise a bow echo, are the following: (1) high amount of moisture in the boundary layer, (2) steep lapse rate in the middle troposphere, (3) low-level lifting mechanism that can initiate and sustain convection, and (4) strong air flow in the troposphere that affects among other things the values of vertical wind shears. The analysis of conditions associated with bow echoes included therefore the determination of parameter values which are shown in Table 1:

Many papers (Klimowski et al. 2003; Cohen et al. 2007; Púčik et al. 2015; to name a few) also proved that the severity of convective events increases, e.g., with the growing values

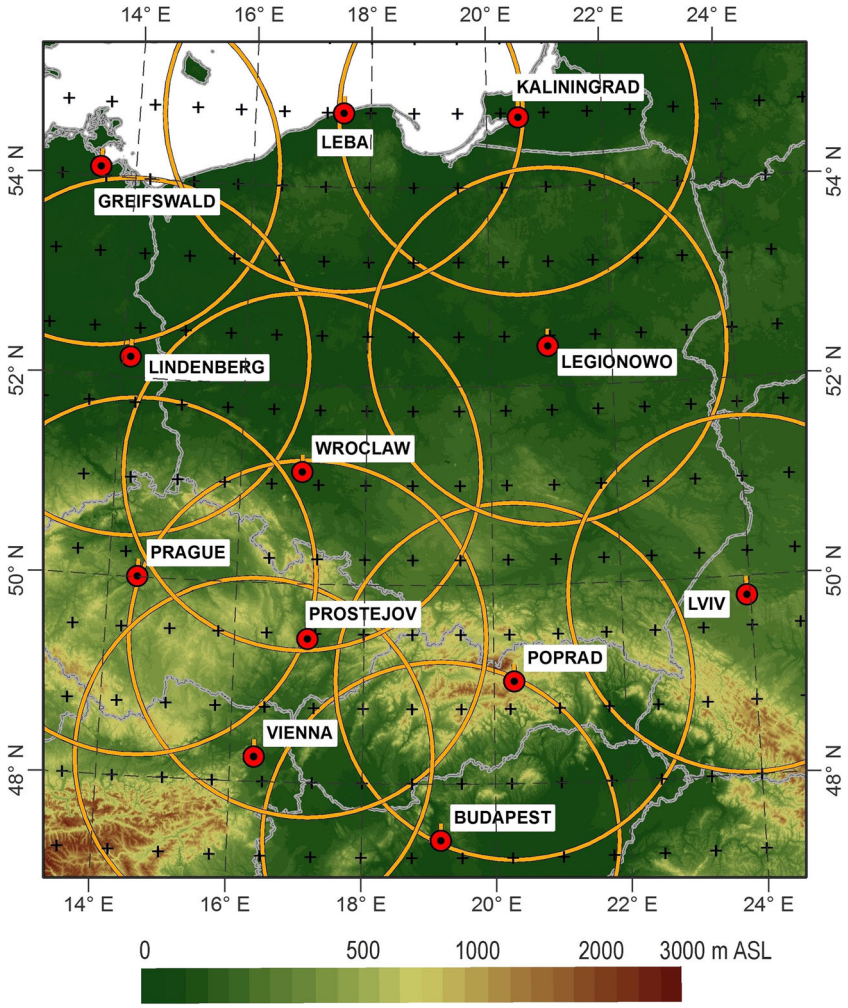

Fig. 2 Exact location of upper air sounding stations (red dots) and Era-Interim grid points (small black crosses). Brown circles represent the 200-km distance from upper air sounding stations

of CAPE and shears. Therefore, we assumed that the development of a bow echo is mostly influenced by the highest values of the shear and CAPE; thus, the grid point with the maximum parameter (one value from all grid points located within or close to the bow echo area) was established to describe the environmental conditions associated with the identified cases. Other thermodynamic indices, such as SBCIN, MLCIN, and DCAPE, were determined exactly for these grid points and time with maximum SBCAPE. To investigate the quality of ERA-Interim reanalysis, we compared the values of the parameters obtained from selected sounding and the nearest grid point (Table 2). A similar method of reanalysis evaluation was used previously by, for example, Gensini et al. (2014) and Taszarek et al. (2018). Additionally, an examination of all bowing episodes was conducted to find recurring surface temperature or moisture patterns.

3 Results

The kinematic and thermodynamic conditions were determined on the basis of 93 upper air soundings for 79 bow echo cases, and as well were based on data from ERA-Interim reanalysis for all 91 identified bow echo cases. Most of the

Table 2 Average differences between upper air and reanalysis data sets (solely for soundings that was selected for identified bow echo cases). We used grid point nearest to the station coordinates

	MLCAPE (J/kg)	SBCAPE (J/kg)	MUCAPE (J/kg)	MLCIN (J/kg)	SBCIN (J/kg)	MUCIN (J/kg)	DCAPE (J/kg)	LLS (m/s)	MLS (m/s)	DLS (m/s)
Mean errors	40	− 311	− 297	− 14.3	5.5	18.3	− 23	− 2.22	− 1.70	− 1.87

analyzed soundings derived from 12 UTC (67). Early morning soundings (06 UTC) accounted for less than 5%. The areas of bow echo cases for which none of the soundings met the assumptions covered mainly north-eastern and south-eastern Poland. These cases usually occurred between 19 and 23 UTC.

3.1 Thermodynamic conditions

The temperature and moisture content in the troposphere have significantly influenced the possibilities of bow echo formation in the warm season in Poland. Ahead of a convective system with a bow echo, the median values of sounding near surface temperature varied from 23.1 °C in transitional months (April, May, September) to 26.6 °C at the peak of the warm season (July). Slightly higher values were observed in the case of 2-m temperature derived from ERA-Interim reanalysis (2mT-ERA). From May to August, the median values then exceeded 25 °C, with a peak in July (almost 27 °C). In transitional months, 2mT-ERA values ahead of a bow echo were usually lower (especially in April—the same as in soundings) (Fig. 3).

The limited spatial and temporal resolution of sounding data caused in some cases that surface temperature and dew point varied greatly between the site of the proximity sounding and the eventual path and occurrence time of the bow echo apex. Synoptic station data showed that just before the bow echo passage, 2-m temperature (2mT-ST) was usually substantially higher both from upper air and reanalysis data (the highest differences were noted for cases that occurred between 14 and 18 UTC in June, July, and August). For cases that occurred at night and in the morning, the maximum 2mT-ST was usually lower than indicated by data from soundings and ERA-Interim reanalysis. It should be emphasized that the tightening of range criterion could eliminate soundings for cases with the highest differences of parameter values. It would undoubtedly reduce the impact on mean and median values (Fig. 3). The noticeable increase of the 2mT-ST ahead of bow echoes suggests that the values of instability indices, computed using both soundings and reanalysis data, can be underestimated, especially for cases between 14 and 18 UTC. It refers particularly to these parameters within which the calculation formula takes into account environmental conditions in the lowest part of the troposphere.

The advection of warm and relatively humid air in the lower troposphere played a considerable role in bow echo development. Median of MIXR for the indentified bow echoes exceeded 11.6 g/kg in the case of the sounding data and reached 12.9 g/kg for the reanalysis data (Fig. 4). The highest values were found in July, coinciding with the results for instance of Klimowski et al. (2003), for severe convective windstorms that occurred over the Central Plains Mid-Mississippi Valley Region in the USA. The research conducted by Taszarek et al. (2017) for parts of Western and Central Europe indicated similar median values for significant tornadoes, but noticeably lower for severe wind gusts (slightly above 10 g/kg).

Apart from thermal and moisture conditions in the boundary layer, mid-tropospheric lapse rates also have a direct impact on the amount of CAPE. An analysis of the bow echo cases indicated that the median of tLR800-500 was slightly higher for reanalysis data and equaled 6.64 °C/km. The month-to-month distribution did not demonstrate significant differences. Only in August, the values were noticeably lower (6.35 °C/km—soundings, 6.42 °C/km—ERA-Interim), but with a large range of variation (especially for soundings) (Fig. 5). These results are consistent with the study of Taszarek et al. (2017) on convective systems generating severe wind gusts and large hail. Burke and Schultz's (2004) research in turn showed slightly higher values for the cool season bow echo cases that occurred in the USA between 1997 and 2001. This may be partly owing to the fact that the temperature lapse rate in their study was computed as a difference between 850 and 500 hPa. The median for LCL varied from 1134 (SBLCL) to 1245 m (MULCL) for soundings and from 812 (SBLCL) to 992 m (MULCL) for ERA-Interim.

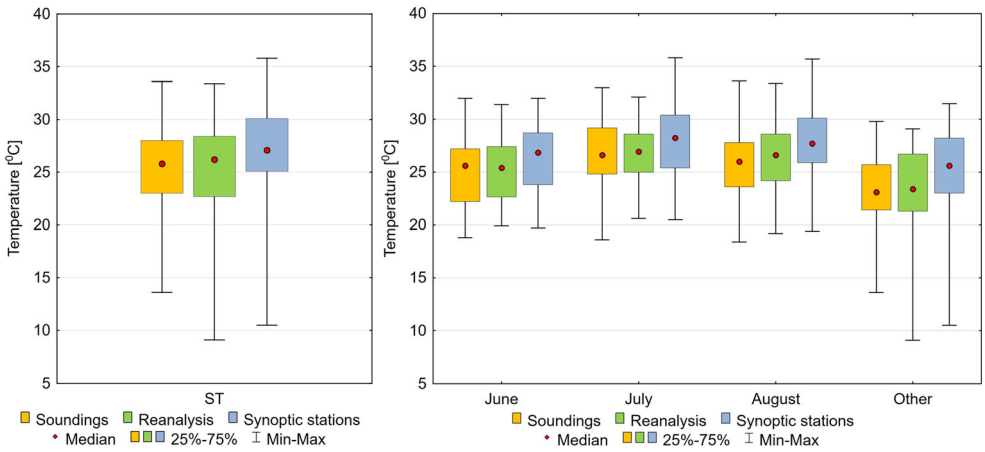

Fig. 3 Box-and-whisker plots of the following: soundings—near surface temperature; reanalysis—2-m temperature; and synoptic stations—maximum 2-m temperature ahead of bow echo (for all cases, on the left; for cases in individual months, on the right). In the analyzed period, 3 bow echo cases occurred in April, 10 in May, 18 in June, 28 in July, 30 in August, and 2 in September

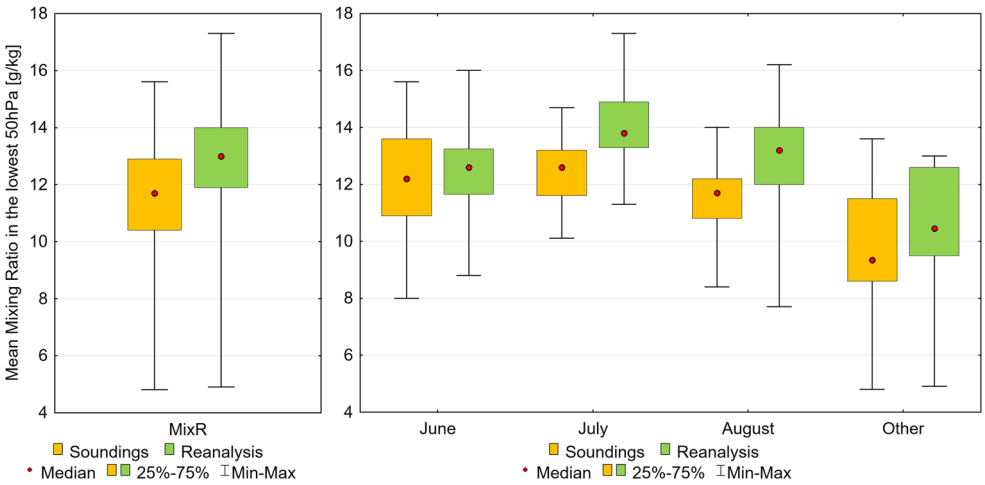

Fig. 4 Box-and-whisker plots of MixR (for all cases, on the left; for cases in individual months, on the right)

The combination of a moist boundary layer and steep mid-tropospheric lapse rate usually resulted in moderate to high CAPE values for identified bow echo cases. The median of SBCAPE equaled to 1594 J/kg (MLCAPE = 1038 J/kg, MUCAPE = 1680 J/kg) for soundings, and to 1622 J/kg (MLCAPE = 1275 J/kg, MUCAPE = 1630 J/kg) for ERA-Interim. However, the maximum values reached as high as 4337 J/kg in the peak of the warm season (Fig. 6). MUCAPE values were usually comparable with SBCAPE. The only exceptions were night and early morning soundings when the occurrence of surface-based inversions induced significant differences, i.e., much larger MUCAPE. It is also worth adding that for those cases which were accompanied by lower temperatures near the surface, and consequently a lower level of thermodynamic instability, the dynamic wind field played a dominant role (usually large values of kinematic parameters). A larger CAPE was usually necessary for cases that occurred in weakly forced environments.

Additional attention should be given to uncertainties in CAPE values between selected soundings and the nearest grid points. For bow echo cases, ERA-Interim underestimates CAPE on average by approximately 311 J/kg for SBCAPE and 297 J/kg for MUCAPE, but overestimates MLCAPE by about 40 J/kg (Table 2). Particularly high differences concerned the cases with a strong boundary layer temperature lapse rate, e.g., strong surface-based inversion or significant drop of temperature with height near the surface. They are probably not well represented by ERA-Interim but significantly influence CAPE values. Grünwald and Brooks (2011) highlighted that capping inversions could also not be sufficiently resolved by NCEP/NCAR (National Centers for Environmental Prediction/National Center for Atmospheric Research). Previous studies showed evidences that for severe thunderstorm, also other reanalyses, such as the North American Regional Reanalysis (NARR), better represent kinematic than thermodynamic variables. Gensini et al. (2014) documented that thermodynamic parameters, such as CAPE, exhibit regional biases and are generally overestimated by NARR reanalysis. They also found large biases and errors in the CIN fields due to the underestimation of temperature inversion strength. In our research, MLCIN were generally underestimated, but SBCIN and MUCIN were overestimated

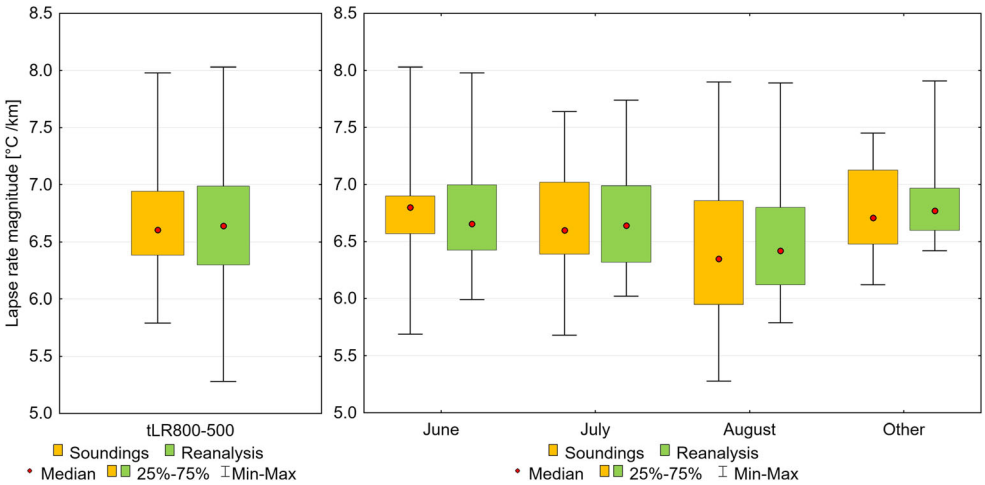

Fig. 5 Box-and-whisker plots of tLR800-500 (for all cases, on the left; for cases in individual months, on the right)

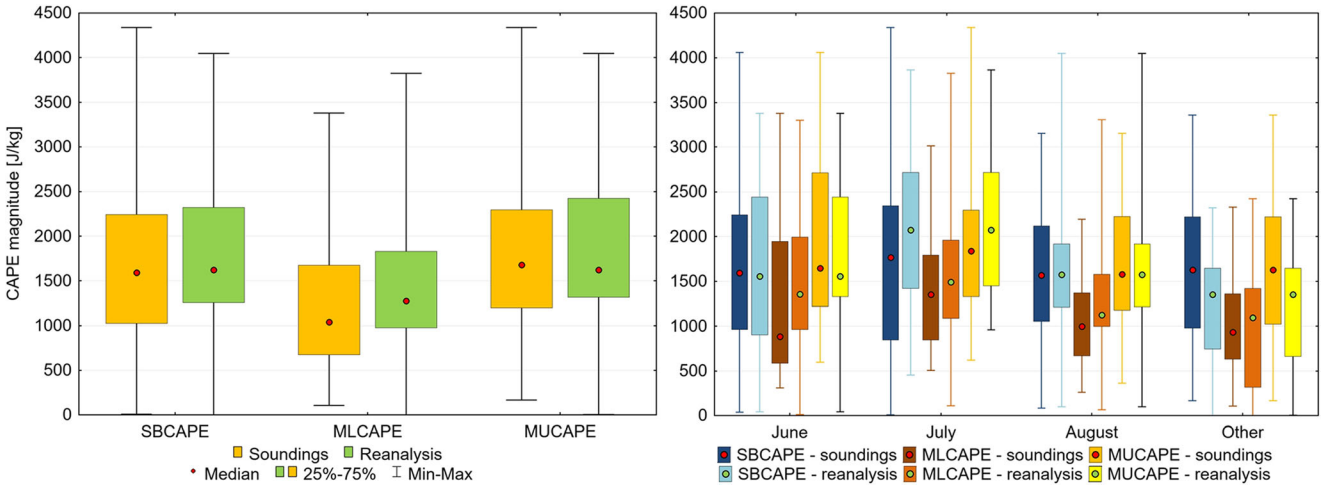

Fig. 6 Box-and-whisker plots of SBCAPE, MLCAPE, and MUCAPE (for all cases, on the left; for cases in individual months, on the right)

(Table 2). Taking into account the ERA-Interim biases and the limitation of sounding data, the median CAPE for identified bow echo cases is expected to be even higher than this from the reanalysis (particularly for SB and MU parcels). Irrespective of the chosen parcel, the median CIN for reanalysis was similar and equaled around 40 J/kg. In case of sounding data, the values varied considerably. The lowest median CIN was found for MU parcel (11 J/kg) and the highest for ML parcel (38 J/kg).

The high vertical temperature gradient and low humidity in the middle troposphere, in turn, created favorable conditions for the development of strong downdrafts. The median DCAPE reached 849 J/kg for soundings and 734 J/kg for ERA-Interim. However, for some bow echoes, DCAPE exceeded 1200 J/kg. This was associated with an increasing potential for strong downdrafts and damaging outflow winds. Evans and Doswell III (2001) and Kuchera and Parker (2006) showed evidences that high values of DCAPE were found usually for events without a large-scale linear forcing mechanism, e.g., when weak-forcing derecho phenomena occurred (Fig. 7).

Differences in CAPE between the parameter values derived from ERA-Interim and from soundings (diff-CAPE) depended on the level from which the air parcel was lifted. Its lowest mean values occurred in the case of the MUCAPE (− 329 J/kg), while the highest (649 J/kg) in the case of the MLCAPE. There was no linear relationship between CAPE values derived from the in situ observations and reanalysis (Fig. 8).

3.2 Kinematic conditions

Bow echoes were usually associated with the presence of strong air flow in the troposphere. Bearing in mind the assumed criteria, jet streams on different levels were observed for nearly 60% of bow echo cases. The upper jet appeared slightly more often than the lower jet. The maximum wind speed within the upper jet reached even more than 50 m/s (for five cases). At the 500 hPa, in turn, the lower jet stream

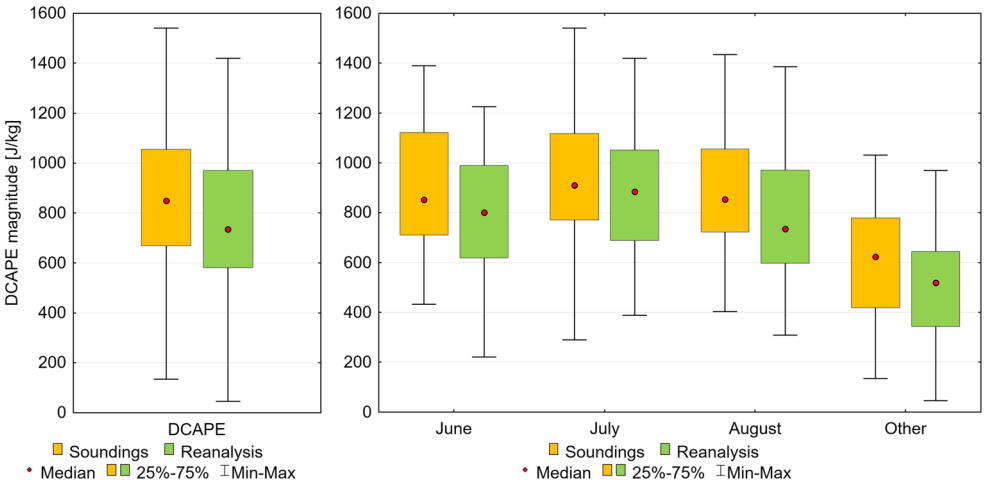

Fig. 7 Box-and-whisker plots of DCAPE (for all cases, on the left; for cases in individual month, on the right)

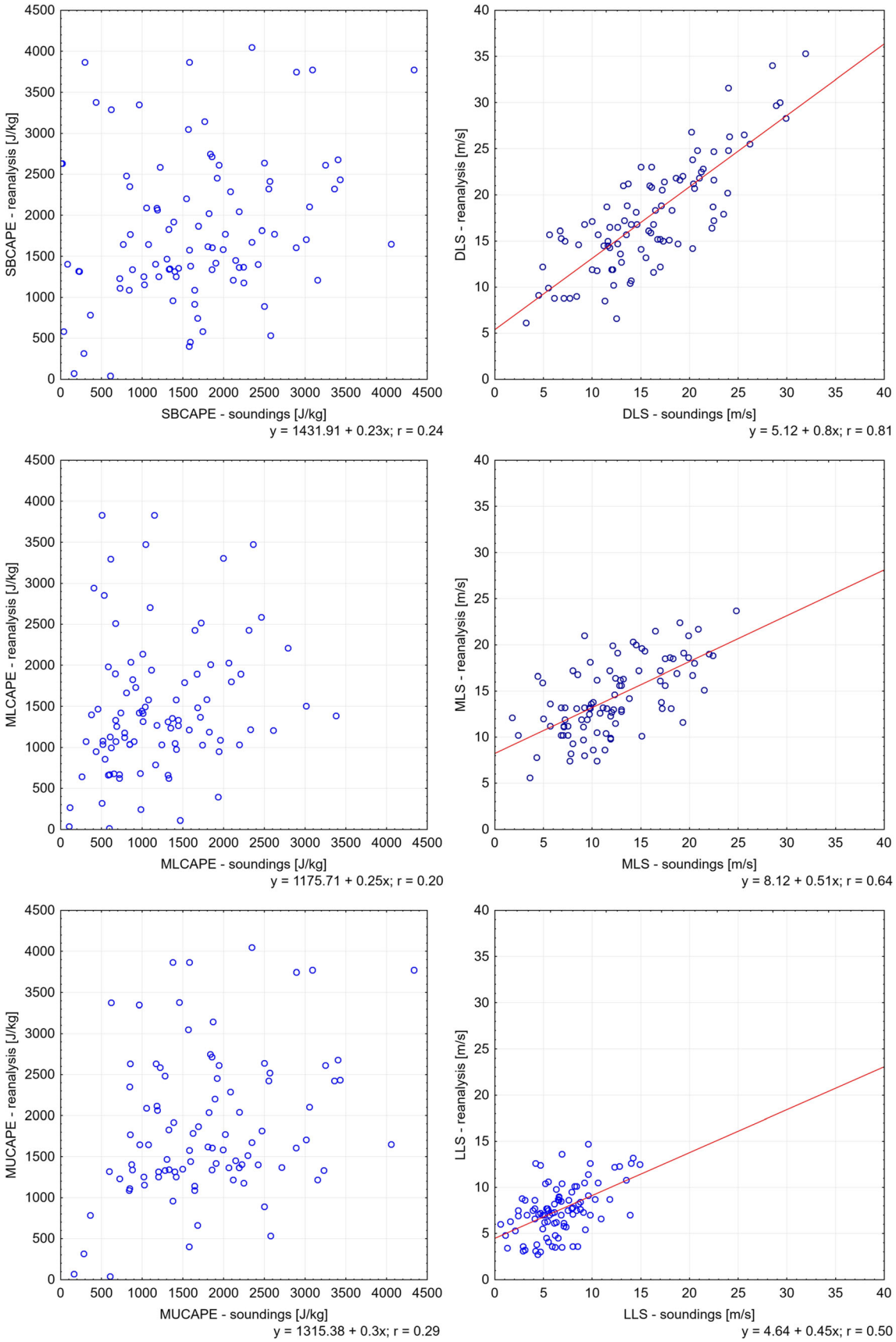

Fig. 8 The differences between CAPE values (on the left) and shear values (on the right) from soundings and ERA-Interim (grid points associated with bow echo areas)

achieved a horizontal speed of more than 35 m/s (for two cases). Taking into consideration bow echo types, virtually all squall line bow echo cases (five out of six) were accompanied by the occurrence of a jet stream. For other types, the percentage of upper or lower jet occurrence ranged from 40% for cell bow echo to 60% for bow echo complex. As shown in Celiński-Mysław and Matuszko (2014), middle and high level jets, augmented by high thermodynamic instability, are conducive to the development of derechoes.

The presence of a jet stream in the middle and upper troposphere contributed to the development of increased vertical wind shear values. It provided a good separation between updrafts and downdrafts, thus contributing to the development of a deep convection effect. It was significant, particularly for cases when low values of thermodynamic parameters occurred. Especially during low CAPE conditions, the DLS magnitude was very important for the spatial arrangement, the maximum size of the convective system (and bow echo), and their longevity. The median value of vertical wind shears (VWS) for identified cases exceeded 15 m/s for DLS (15.9 m/s, soundings; 16.8 m/s, ERA-Interim), and was approximately equal to 12.5 m/s for MLS (11.9 m/s, soundings; 13.2 m/s, ERA-Interim) and to 7 m/s for LLS (6.3 m/s, soundings; 7.5 m/s, ERA-Interim). However, for some cases, DLS reached values > 30 m/s, MLS > 20 m/s, and LLS > 15 m/s. VWS did not show substantial differences between particular months (Fig. 9). A slightly lower value was observed solely in May, especially for DLS and MLS. The higher shears in September should be treated with caution owing to the low number of cases in this month. Particular attention should also be paid to the uncertainties in the VWS values between selected soundings and the nearest grid points. A comparison of shear values pointed out that for bow echo cases, ERA-Interim underestimates them by approximately 2.2 m/s for LLS, 1.7 m/s for MLS, and 1.9 m/s for DLS (Table 2). Therefore, it can be assumed that mean/median VWS values for bow echo areas were even higher (especially in the case of LLS).

Differences between the parameter values derived from ERA-Interim (grid points from bow echo areas) and from soundings (diff-SHEAR) varied with the selected vertical wind shear. Its lowest mean values occurred for LLS (0.99 m/s), while the highest (2.15 m/s) for MLS. Mean diff-SHEAR for DLS were noticeably lower than in the case of MLS, although this parameter usually assumes significantly higher values. Shear values derived from the in situ observations and reanalysis products showed different correlation between each other. The Pearson's correlation coefficient ranged from 0.50 (LLS) to 0.81 (DLS) (Fig. 8).

3.3 Parameter combinations

Scatterplots for MLS and DLS vs SBCAPE confirm that bow echo events happen over a very wide range of parameter values. The warm season cases occurred both in weakly forced environments and developed in dynamic synoptic patterns with low instability as is consistent with, e.g., Evans and Doswell III (2001). For ERA-Interim, most of the cases were accompanied by SBCAPE exceeding 1000 J/kg and MLS or DLS above 10 m/s (Fig. 10). There were almost no events in low CAPE and low shear. For sounding data, an increased number of events with MLS and DLS below 10 m/s were observed (more cases with low LLS). This can be explained by the poor spatial resolution of this data. In many cases, soundings defined kinematic and thermodynamic conditions not exactly for the bow echo area, but at a considerable distance from it (not exceeding the assumed 200 km), which could account for the underestimated values of the parameters.

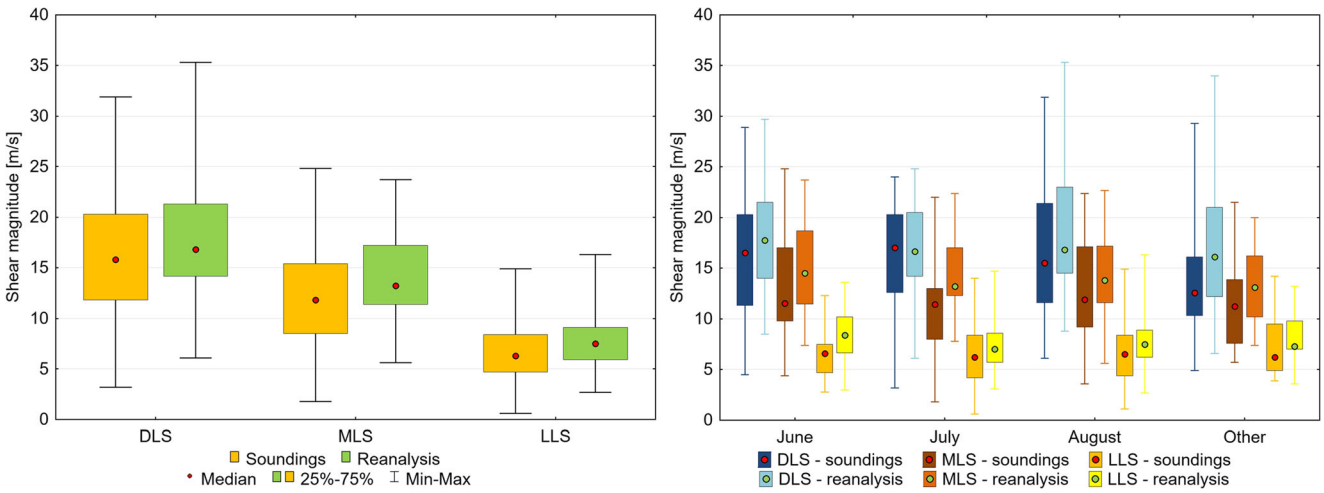

Fig. 9 Box-and-whisker plots of DLS, MLS, and LLS (for all cases, on the left; for cases in individual months, on the right)

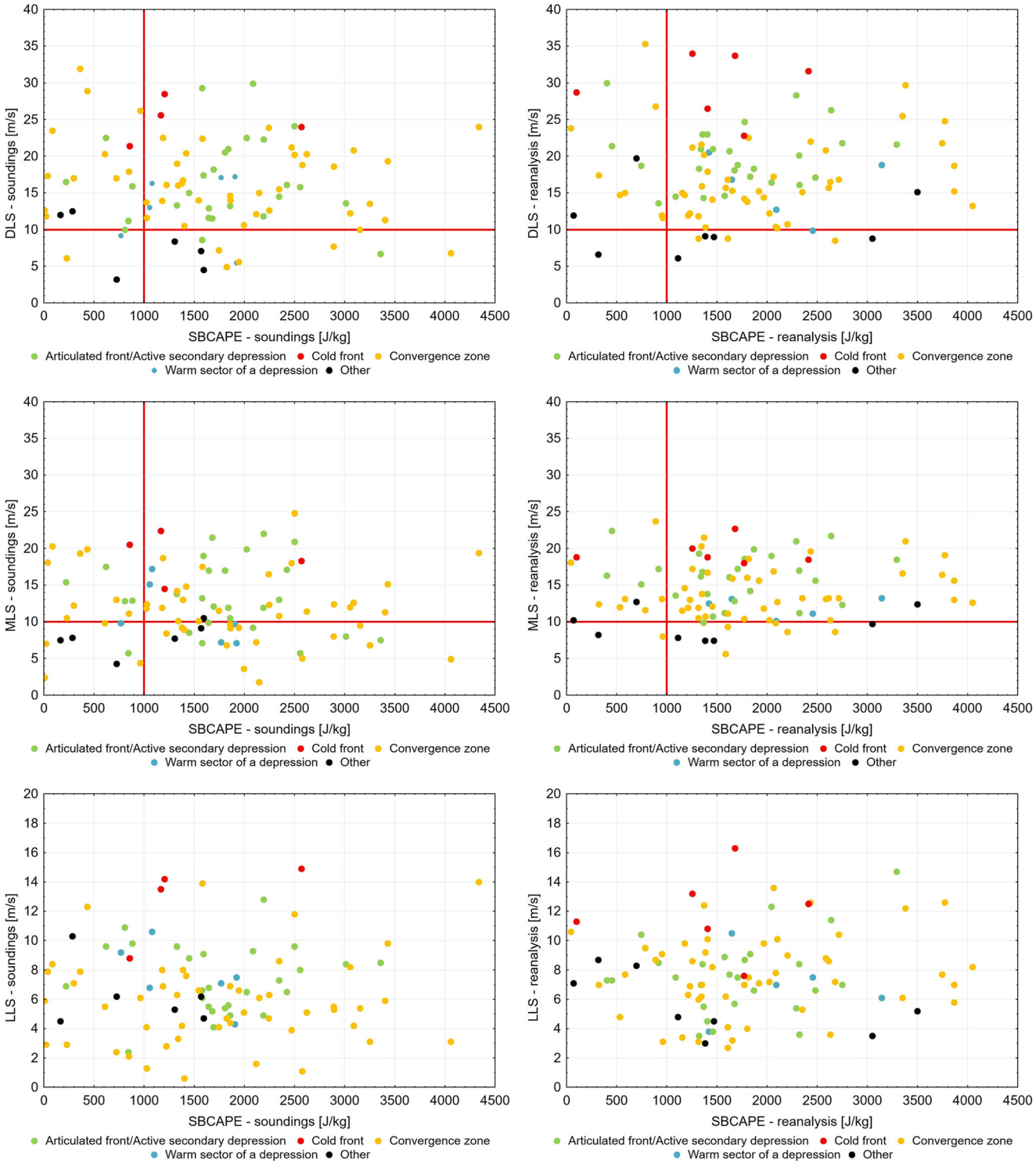

Fig. 10 Scatterplots of DLS, MLS, and LLS vs. SBCAPE. Each plot is classified by an environment of bow echo development

Analyzing these relationships with respect to the environment of bow echo development, we noticed high shear values for all cases which formed on the cold front, but quite low for many cases that developed in an environment without a large-scale system supporting convection (other) (Fig. 10). There is a clear absence of trends for other groups. Probably additional relations between CAPE and shears would be noticed using the division of bow echo cases according to the criteria of their severity such as the number of severe wind reports, maximum wind gusts, or caused damage.

4 Discussion

Warm season bow echo windstorms can develop over Poland in various environments. In so far as the cool season, bow echoes are characterized primarily by strong flow in the troposphere with low instability (e.g., Clark 2011; Gatzen et al. 2011; Celiński-Mysław and Matuszko 2014) as our results present the warm season cases can form both in weakly and strongly forced environments. Thermodynamic and kinematic parameters differ substantially for individual cases. However, the values of kinematic parameters are not so large as in the cool half of the year when bow echoes develop as a result of a squall line transformation, which forms on the cold front of deep low-pressure systems (Gatzen et al. 2011; Celiński-Mysław and Matuszko 2014).

As indicated by Celiński-Mysław and Palarz (2017), bow echo thunderstorms in Poland occur most frequently in summer (May/June to August), with a pronounced diurnal cycle (predominantly between 13 and 21 UTC). A significant temperature growth before a bow echo occurrence and a rapid drop after a bow echo passage were also observed by, among others, Adams-Selin and Johnson (2010), Hamid (2012), and Celiński-Mysław and Matuszko (2014). A temperature increase ahead of the convective system with a bow echo (particularly in the afternoon), advection relatively humid air in the lower troposphere, and steep mid-tropospheric lapse rate had a direct impact on the amount of CAPE.

The wide range of CAPE and shear found for bow echoes overlaps with the results obtained by, among others, Evans and Doswell III (2001), Klimowski et al. (2003), or Cohen et al. (2007). They indicated that a severe long-lived bow echo can form even when CAPE is low. The results, however, vary considerably depending on the areas of occurrence. It is worth pointing out that markedly higher values of CAPE for bow echoes are identified over the USA compared with values for Poland. The median of MUCAPE in our study was not much higher than the mean MUCAPE for cool season bow echoes in the USA (1366 J/kg—Burke and Schultz 2004). Previous studies have demonstrated that the average value of SBCAPE for warm season severe wind bow echoes in the USA exceeded 3100 J/kg (Klimowski et al. 2003). Significant differences in CAPE values for severe wind events between the results obtained in the USA and Europe were pointed out also by, inter alia, Púčik et al. (2015) (for the years 2007–2013). They found that median MUCAPE of severe wind gust cases in Central Europe equaled 549 J/kg, while in the USA, it exceeded 1900 J/kg (Kuchera and Parker 2006). However, it should also be emphasized that median values of MUCAPE and DCAPE were much higher for identified bow echoes in Poland in comparison to those (severe wind events) demonstrated by Púčik et al. (2015) for Central Europe (including Poland). Higher values of DCAPE, resulted by the vertical temperature gradient and low humidity in the middle troposphere, were conducive to the formation of colder downdrafts and a stronger cold pool, thus increasing potential for damaging outflow winds (Gilmore and Wicker 1998; James et al. 2006). James et al. (2006) concluded also that strengthening of the cold pool might be the trigger that initiated the development of coherent bowing segments generated within a convective line.

The increased values of CAPE and DCAPE are usually necessary for bow echo development in the warm season, but not sufficient. Bow echo thunderstorm formation is also strongly affected by the presence of fast flow from mid to upper level. This enhances the possibility of severe wind gusts formation via vertical transfer of momentum in downdrafts. The jet stream boosts the dynamic of the troposphere and contributes to the increase in shear values, ensuring good separation between updrafts and downdrafts, and thus contributes to the formation of severe convective storms. The presence of mid-level and high-level jets had some influence also on the movement speed of convective systems and extended their life, thus allowing them to travel over long distances and frequently to cover large parts of Poland. The importance of fast flow in the troposphere for bow echo and derecho development was proved also in the earlier studies (Coniglio et al. 2004; Cohen et al. 2007; Celiński-Mysław and Matuszko 2014; Guastini and Bosart 2016). Cohen et al. (2007) confirmed also previous findings that situations in which deep layer shear is large and in the same direction as the deep layer mean wind favor fast forward-propagating and severe MCSs. Coniglio et al. (2004), in turn, indicated that a convective system causing derecho tends to decay as it moves into environments with less instability and smaller deep-layer shear, as we also observed (not shown).

Referring to the shear values, the study conducted by Burke and Schultz (2004) indicated higher mean/median for bow echo cases that occurred over the continental USA than in Poland. This research, however, was focused solely on cool season bow echo cases. As demonstrated by studies of Celiński-Mysław and Matuszko (2014) and Gatzen et al. (2011), the development of MCSs with bow echoes in the cool season in Central Europe was also accompanied by high wind shear values (higher than obtained in this research). In the above-mentioned studies, wind speed within the jet stream exceeded 70 m/s and DLS reached values even higher than 50 m/s. Furthermore, our results also confirm the findings of Púčik et al. (2015) that severe wind events in Central Europe typically occur with high DLS. As shown in the research, the median DLS was around 16.1 m/s for warm season events, and 33.2 m/s for cool season events. Similarly, large differences were indicated in the case of median LLS (6.6 m/s for the warm season, 18.1 for the cool season).

It is also important to underline the limitations of the datasets. Large diff-CAPE and diff-SHEAR suggest the limited applicability of the upper air sounding data in the analysis of conditions accompanying the occurrence of MCSs which are remote in time and space from the point of sounding. Many previous studies

also paid attention to this problem (Burke and Schultz 2004; Cohen et al. 2007; Potvin et al. 2010; to name a few). As indicated in Potvin et al. (2010), soundings collected further than 80 km from thunderstorm events are more representative of the larger-scale environment than of the storm environment. Beebe (1958), in turn, showed that soundings performed very close in time and space to tornadoes had a significantly different vertical structure in comparison with those taken several hours earlier. Potvin et al. (2010) also concluded that soundings performed closer to the tornado (closer than 40 km) tend to be less representative owing to the convective feedback processes, e.g., anvil shadow, cold outflow, and precipitation. In order to reduce the influence of the distance of soundings from derecho/bow echo areas as well as to better represent the thermodynamic environment in which bow echoes formed, Evans and Doswell III (2001) and Burke and Schultz (2004) have modified radiosonde data by using synoptic station observations taken immediately ahead of the convective system. Nowotarski and Markowski (2016), in turn, proved that low-level shear increases in proximity to supercell thunderstorms owing to low-level inflow acceleration by the storm updraft. They also showed that the cloud shading and boundary layer convection affect the decreased magnitude of CAPE and LCL near the storm.

A better ERA-Interim resolution, both spatial (3 upper air sounding stations compared to 72 grid points over Poland) and temporal (resolution of the reanalysis data is 6 h, while sounding data from most of the stations are available every 12 h) is an undoubted strength of this dataset. However, to be borne in mind are its potential biases and errors for rare events (Grünwald and Brooks 2011; Allen and Karoly 2014; Gensini et al. 2014; Westermayer et al. 2016b), such as bow echo cases (Table 2), particularly for thermodynamic parameters. Gensini et al. (2014) who utilized the North American Regional Reanalysis (NARR) showed that the thermodynamic variables suffer particularly from errors originating in low-level moisture fields. Similar results were presented by Westermayer et al. (2016b) for ERA-Interim and CFS reanalyses. Both reanalysis products showed that deep layer shear (DLS) is well represented for thunderstorm situations over Central Europe, while for MLCAPE, there is less correlation between the observations and both reanalysis datasets. Also, Allen and Karoly (2014) demonstrated low-level thermodynamic biases for Era-Interim which are particularly problematic for variables that rely on vertical integration (e.g., CAPE or CIN). Small biases in the low-level temperature and moisture fields may, in fact, cause large differences in derivatives parameters such as CAPE.

5 Conclusions

In this study, we have investigated the formation conditions of convective systems with a bow echo in the warm season in Poland. Our results are broadly consistent with previous findings on severe wind events in Central Europe (such as Púčik et al. 2015; Taszarek et al. 2017) but deviate significantly from the results obtained for the USA. Likewise, as in the study by Pucik et al. (2015), high wind events (such as for example convective systems with a bow echo) occurred in Poland with much lower CAPE, but with more similar DLS and MLS (in comparison to, for instance, Klimowski et al. 2003; Kuchera and Parker 2006).

The results of our research indicate that there is a relatively wide range of shear and instability environments associated with bow echoes over Poland. The identified cases occurred both in weakly forced environments, and as well developed in dynamic synoptic patterns with low instability. We have also found cases with strong instability and significantly increased shear values. Similarly to the results obtained by Celiński-Mysław and Matuszko (2014), such conditions usually caused the occurrence of a warm season derecho. The study concluded, however, that moderate to high CAPE and increased values of MLS and DLS which support organized convection are particularly conducive to the development of this phenomenon. Additionally, as indicated by our previous research (Celiński-Mysław and Palarz 2017), most bow echo cases are associated with convective systems which had formed in the convergence zone or in an articulated atmospheric front with a secondary active depression, and so knowledge of these synoptic development environments and kinematic and thermodynamic variables values can be used to improve forecasts for convective warm season straight-line wind events (bow echo, derecho, etc.) for Poland and Central Europe.

Results obtained for bow echoes show also some significant differences between reanalysis and soundings data. Although ERA-Interim provides higher spatial and temporal resolution, it sometimes deviates quite strongly from the real state of the atmosphere. Thus, when analyzing the environments of severe convective weather events (particularly thermodynamic conditions), sounding and reanalysis data should be utilized in parallel.

Our findings should be further investigated based on a longer period, as well as by shorter time intervals of the data, and better spatial resolution (e.g., realization of downscaling through mesoscale models). A greater number than the present 91 bow echo cases will probably reduce potential biases and make it possible to obtain more robust results from statistical analyses. Follow-up research should also consider the values of additional convective parameters associated with bow echoes in Poland and Central Europe or look for the effects of the type of surface and the orography on the possibilities of its formation. It is also worth dividing bow echo cases according to the intensity criterion (amount of damage, number of reports, etc.) which probably could make it possible to find additional relations between bow echo events and their environment of formation.

Acknowledgements The authors thank the Polish Institute of Meteorology and Water Management – National Research Institute for providing radar data allowing us to identify bow echo cases and the ECMWF for providing the ERA-Interim reanalysis data.

Funding information This study was possible in part due to Jagiellonian University grants (K/DSC/004751).

References

Adams-Selin RD, Johnson RH (2010) Mesoscale surface pressure and temperature features associated with bow echoes. Mon Weather Rev 138:212–227. https://doi.org/10.1175/2009MWR2892.1

Allen JT, Karoly DJ (2014) A climatology of Australian severe thunderstorm environments 1979–2011: inter-annual variability and ENSO influence. Int J Climatol 34:81–97. https://doi.org/10.1002/joc.3667

Atkins NT, St Laurent M (2009) Bow echo mesovortices. Part I: processes that influence their damaging potential. Mon Weather Rev 137:1497–1513. https://doi.org/10.1175/2008MWR2649.1

Beebe RG (1958) Tornado proximity soundings. Bull Am Meteorol Soc 39:195–201

Blumberg WG, Halbert KT, Supinie TA, Marsh PT, Thompson RL, Hart JA (2017) SHARPpy: an open-source sounding analysis toolkit for the atmospheric sciences. Bull Am Meteor Soc 98:1625–1636. https://doi.org/10.1175/BAMS-D-15-00309.1

Brooks HE, Doswell CA, Cooper J (1994) On the environments of tornadic and nontornadic mesocyclones. Weather Forecast 9:606–618. https://doi.org/10.1175/1520-0434(1994)009<0606:OTEOTA>2.0.CO;2

Brooks HE, Lee JW, Craven JP (2003) The spatial distribution of severe thunderstorm and tornado environments from global reanalysis. Atmos Res 67-68:73–94. https://doi.org/10.1016/S0169-8095(03)00045-0

Burke PC, Schultz DM (2004) A 4-Yr climatology of cold-season Bow echoes over the continental United States. Weather Forecast 19:1061–1074. https://doi.org/10.1175/811.1

Celiński-Mysław D, Matuszko D (2014) An analysis of the selected cases of derecho in Poland. Atmos Res 149:263–281. https://doi.org/10.1016/j.atmosres.2014.06.016

Celiński-Mysław D, Palarz A (2017) The occurrence of convective systems with a bow echo in warm season in Poland. Atmos Res 193:26–35. https://doi.org/10.1016/j.atmosres.2017.04.015

Chen GT-J, Wang C-C, Chou H-C (2007) Case study of a bow echo near Taiwan during wintertime. J Meteorol Soc Jpn 85:233–253. https://doi.org/10.2151/jmsj.85.233

Clark MR (2011) Doppler radar observations of mesovortices within a cool-season tornadic squall line over the UK. Atmos Res 193:26–35. https://doi.org/10.1016/j.atmosres.2010.09.007

Cohen AE, Coniglio MC, Corfidi SF, Corfidi SJ (2007) Discrimination of mesoscale convective system environments using sounding observations. Weather Forecast 22:1045–1062. https://doi.org/10.1175/WAF1040.1

Coniglio MC, Stensrud DJ, Richman MB (2004) An observational study of derecho-producing convective storms. Weather Forecast 19:320–337. https://doi.org/10.1175/1520-0434(2004)019<0320:AOSODC>2.0.CO;2

Dee DP, Uppala SM, Simmons J, Berrisford P, Poli P, Kobayashi S, Andrae U, Balmaseda M, Balsamo G, Bauer P, Bechtold P, Beljaars CM, van de Berg L, Bidlot J, Bormann N, Delsol C, Dragani R, Fuentes M, Geer J, Haimberger L, Healy S, Hersbach H, Hólm EV, Isaksen L, Kållberg P, Köhler M, Matricardi M, Mcnally P, Monge-Sanz BM, Morcrette JJ, Park BK, Peubey C, de Rosnay P, Tavolato C, Thépaut JN, Vitart F (2011) The ERA-interim reanalysis: configuration and performance of the data assimilation system. Q J R Meteorol Soc 137:553–597. https://doi.org/10.1002/qj.828

Devajyoti D, Diganta KS, Sanjay S (2014) A multisensor analysis of the life cycle of bow echo over Indian region. Int J Atmos Sci 2014:1–9. https://doi.org/10.1155/2014/207064

Development Core Team R (2008) R: a language and environment for statistical computing. R Foundation for Statistical Computing, Vienna http://www.R-project.org. Accessed 10 June 2018

Evans JS, Doswell CA III (2001) Examination of derecho environments using proximity soundings. Weather Forecast 16:329–342. https://doi.org/10.1175/1520-0434(2001)016,0329:EODEUP.2.0.CO;2

French AJ, Parker MD (2014) Numerical simulations of bow echo formation following a squall line-supercell merger. Mon Weather Rev 142:4791–4822. https://doi.org/10.1175/MWR-D-13-00356.1

Fujita TT (1978) Manual of downburst identification for Project Nimrod. Satellite and Mesometeorology Research Paper No. 156, pp 104. Available from Department of Geophysical Sciences, University of Chicago, Chicago

Gatzen C (2013) Warm-season severe wind events in Germany. Atmos Res 123:197–205. https://doi.org/10.1016/j.atmosres.2012.07.017

Gatzen C, Púčik T, Ryva D (2011) Two cold-season derechoes in Europe. Atmos Res 100:740–748. https://doi.org/10.1016/j.atmosres.2010.11.015

Gensini VA, Mote TL, Brooks HE (2014) Severe-thunderstorm reanalysis environments and collocated radiosonde observations. J Appl Meteorol Climatol 53:742–751. https://doi.org/10.1175/JAMC-D-13-0263.1

Gilmore MS, Wicker LJ (1998) The influence of midtropospheric dryness on supercell morphology and evolution. Mon Weather Rev 126:943–958. https://doi.org/10.1175/1520-0493(1998)126<0943:TIOMDO>2.0.CO;2

Grünwald S, Brooks HE (2011) Relationship between sounding derived parameters and the strength of tornadoes in Europe and the USA from reanalysis data. Atmos Res 100:479–488. https://doi.org/10.1016/j.atmosres.2010.11.011

Guastini CT, Bosart LF (2016) Analysis of a progressive derecho climatology and associated formation environments. Mon Weather Rev 144:1363–1382. https://doi.org/10.1175/MWR-D-15-0256.1

Hamid K (2012) Investigation of the passage of the derecho in Belgium. Atmos Res 107:86–105. https://doi.org/10.1016/j.atmosres.2011.12.013

James RP, Markowski PM, Fritsch JM (2006) Bow echo sensitivity to ambient moisture and cold Pool strength. Mon Weather Rev 134:950–964. https://doi.org/10.1175/MWR3109.1

Johns RH, Doswell CA III (1992) Severe local storms forecasting. Weather Forecast 7:588–612. https://doi.org/10.1175/1520-0434(1992)007,0588:SLSF.2.0.CO;2

Johns RH, Hirt WD (1987) Derechos: widespread convectively induced wind storms. Weather Forecast 2:32–49. https://doi.org/10.1175/1520-0434(1987)002<0032:DWCIW>2.0.CO;2

Kaltenboeck R, Steinheimer M (2015) Radar-based severe storm climatology for Austria complex orography related to vertical wind shear and atmospheric instability. Atmos Res 158-159:216–230. https://doi.org/10.1016/j.atmosres.2014.08.006

Kerr BW, Darkow GL (1996) Storm-relative winds and helicity in the tornadic thunderstorm environment. Weather Forecast 11:

489–505. https://doi.org/10.1175/1520-0434(1996)011<0489:SRWAHI>2.0.CO;2

King AT, Kennedy AD (2018) North American supercell environments in atmospheric reanalysis and RUC-2. J Appl Meteor Climatol Published Online:19. https://doi.org/10.1175/JAMC-D-18-0015.1

Klimowski BA, Bunkers MJ, Hjelmfelt MR, Covert JN (2003) Severe convective windstorms over the northern High Plains of the United States. Weather Forecast 18:502–519. https://doi.org/10.1175/1520-0434(2003)18<502:SCWOTN>2.0.CO;2

Klimowski BA, Hjelmfelt MR, Bunkers MJ (2004) Radar observations of the early evolution of bow echoes. Weather Forecast 19:727–734. https://doi.org/10.1175/1520-0434(2004)019<0727:ROOTEE>2.0.CO;2

Kolendowicz L, Taszarek M, Czernecki B (2017) Atmospheric circulation and sounding-derived parameters associated with thunderstorm occurrence in Central Europe. Atmos Res 191:101–114. https://doi.org/10.1016/j.atmosres.2017.03.009

Kuchera EL, Parker MD (2006) Severe convective wind environments. Weather Forecast 21:595–612. https://doi.org/10.1175/WAF931.1

Lopez JM (2007) A Mediterranean derecho: Catalonia (Spain), 17th august 2003. Atmos Res 83:272–283. https://doi.org/10.1016/j.atmosres.2005.08.008

Mathias L, Ermert V, Kelemen FD, Ludwig P, Pinto JG (2017) Synoptic analysis and Hindcast of an intense Bow Echo in Western Europe: the 9 June 2014 storm. Weather Forecast 32:1121–1141. https://doi.org/10.1175/WAF-D-16-0192.1

Miller PW, Mote TL (2018) Characterizing severe weather potential in synoptically weakly forced thunderstorm environments. Nat Hazards Earth Syst Sci 18:1261–1277. https://doi.org/10.5194/nhess-18-1261-2018

Nowotarski CJ, Markowski PM (2016) Modifications to the near-storm environment by simulated supercell thunderstorms. Mon Weather Rev 144:273–293. https://doi.org/10.1175/MWR-D-15-0247.1

Peng X, Zhang R, Wang H (2013) Kinematic features of bow echo in southern China observed with Doppler radar. Adv Atmos Sci 30:1535–1548. https://doi.org/10.1007/s00376-012-2108-6

Potvin CK, Elmore KL, Weiss SJ (2010) Assessing the impacts of proximity sounding criteria on the climatology of significant tornado environments. Weather Forecast 25:921–930. https://doi.org/10.1175/2010WAF2222368.1

Przybylinski RW (1995) The bow echo observations, numerical simulations and severe weather detection methods. Weather Forecast 10:203–218. https://doi.org/10.1175/1520-0434(1995)010<0203:TBEONS>2.0.CO;2

Púčik T, Francova M, Ryva D, Kolar M, Ronge L (2011) Forecasting challenges during the severe weather outbreak in Central Europe on 25 June 2008. Atmos Res 100:680–704. https://doi.org/10.1016/j.atmosres.2010.11.014

Púčik T, Groenemeijer P, Ryva D, Kolar M (2015) Proximity soundings of severe and nonsevere thunderstorm in Central Europe. Mon Weather Rev 143:4805–4821. https://doi.org/10.1175/MWR-D-15-0104.1

Punkka A-J, Teittinen J, Johns RH (2006) Synoptic and mesoscale analysis of a high latitude derecho-severe thunderstorm outbreak in Finland on 5 July 2002. Weather Forecast 21:752–763. https://doi.org/10.1175/WAF953.1

Ribaud J-F, Bousquet O, Coquillat S (2016) Relationships between total lighting activity, microphysics and kinematics during the 24 September 2012 HyMeX bow-echo system. Q J R Meteorol Soc 142:298–309. https://doi.org/10.1002/qj.2756

Romero R, Gaya M, Doswell CA III (2007) European climatology of severe convective storm environmental parameters: a test for significant tornado events. Atmos Res 83:389–404. https://doi.org/10.1016/j.atmosres.2005.06.011

Rotunno R, Klemp JB, Weisman ML (1988) A theory for strong, long-lived squall lines. J Atmos Sci 45:463–485. https://doi.org/10.1175/1520-0469(1988)045<0463:ATFSLL>2.0.CO;2

Schoen JM, Ashley WS (2011) A climatology of fatal convective wind events by storm time. Weather Forecast 26:109–121. https://doi.org/10.1175/2010WAF2222428.1

Taszarek M, Kolendowicz L (2013) Sounding-derived parameters associated with tornado occurrence in Poland and universal tornadic index. Atmos Res 134:186–197. https://doi.org/10.1016/j.atmosres.2013.07.016

Taszarek M, Brooks HE, Czernecki B (2017) Sounding-derived parameters associated with convective hazards in Europe. Mon Weather Rev 145:1511–1528. https://doi.org/10.1175/MWR-D-16-0384.1

Taszarek M, Brooks HE, Czernecki B, Szuster P, Fortuniak K (2018) Climatological aspects of convective parameters over Europe: a comparison of ERA-interim and sounding data. J Clim 31:4281–4308. https://doi.org/10.1175/JCLI-D-17-0596.1

Torres Brizuela M, Vidal R, Skabar YG, Nicolini M, Vidal L (2011) Analisis del entorno sinoptico asociado con eventos de bow-echo en la provincia de Buenos Aires. Meteorologica 36:3–17

Trapp RJ, Weisman ML (2003) Low-level mesovortices within squall lines and bow echoes. Part II: their genesis and implications. Mon Weather Rev 131:2804–2823. https://doi.org/10.1175/1520-0493(2003)131<2804:LMWSLA>2.0.CO;2

Wakimoto RM, Murphey HV, Davis CA, Atkins NT (2006a) High winds generated by Bow echoes. Part II: the relationship between the Mesovortices and damaging straight-line winds. Mon Weather Rev 134:2813–2829. https://doi.org/10.1175/MWR3216.1

Wakimoto RM, Murphey HV, Nester A, Jorgensen DP, Atkins NT (2006b) Highwinds generated by bow echoes. Part I: overview of the Omaha bow echo 5 July 2003 storm during BAMEX. Mon Weather Rev 134:2793–2812

Weisman ML (1992) The role of convectively generated rear-inflow jets in the evolution of long-lived mesoconvective systems. J Atmos Sci 49:1826–1847. https://doi.org/10.1175/1520-0469(1992)049,1826:TROCGR.2.0.CO;2

Weisman ML (1993) The genesis of severe, long-lived bow echoes. J Atmos Sci 50:645–670. https://doi.org/10.1175/1520-0469(1993)050<0645:TGOSLL>2.0.CO;2

Weisman ML, Klemp JB (1982) The dependence of numerically simulated convective storms on vertical wind shear and buoyancy. Mon Weather Rev 110:504–520. https://doi.org/10.1175/1520-0493(1982)110,0504:TDONSC.2.0.CO;2

Weisman ML, Trapp RJ (2003) Low-level mesovortices within squall lines and bow echoes. Part I: overview and sensitivity to environmental vertical wind shear. Mon Weather Rev 131:2779–2803. https://doi.org/10.1175/1520-0493(2003)131<2779:LMWSLA>2.0.CO;2

Westermayer AT, Groenemeijer P, Pistotnik G, Sausen R, Faust E (2016a) Identification of favorable environments for thunderstorms in reanalysis data. Meteorol Z 26:59–70. https://doi.org/10.1127/metz/2016/0754

Westermayer AT, Púčik T, Groenemeijer P, Tijssen L (2016b) Comparison of sounding observations and reanalysis of thunderstorm environments. Eighth European Conf. on Severe Storms. Austria, European Severe Storms Laboratory, Wiener Neustadt http://meetingorganizer.copernicus.org/ECSS2015/ECSS2015-136-1.pdf. Accessed 10 April 2018

Wheatley DM, Trapp RJ, Atkins NT (2006) Radar and damage analysis of severe bow echoes observed during BAMEX. Mon Weather Rev 134:791–806. https://doi.org/10.1175/MWR3100.1

Xu X, Xue M, Wang Y (2015) Mesovortices within the 8 May 2009 bow echo over the Central United States: analyses of the characteristics and evolution based on Doppler radar observations and a high-resolution model simulation. Mon Weather Rev 143:2266–2290. https://doi.org/10.1175/MWR-D-14-00234.1

Zhao L, Wang S-Y, Jin J, Clark AJ (2015) Weather research and forecasting model simulations of a rare springtime bow echo near the great salt Lake, USA. Meteorol Appl 22:301–313. https://doi.org/10.1002/met.145